SITE-SPECIFIC MEMBRANE PARTICLE ARRAYS IN MAGNESIUM-DEPLETED *ESCHERICHIA COLI*

RICHARD L. WEISS

From the Biological Laboratories, Harvard University, Cambridge, Massachusetts 02138. Dr. Weiss's present address is the Department of Medical Microbiology, College of Medicine, University of California, Irvine, Irvine, California 92717.

ABSTRACT

The ultrastructure and polypeptide composition of a novel membrane junction in magnesium-starved *Escherichia coli* are described in this report. Freeze-fracture replicas reveal the junction as a site-specific membrane particle array with four fracture faces. Each junction consists of a cell membrane, a midline zone and a coupled membrane. Membrane particles associated with the junction extend from the hydrophobic region of the cell membrane across the hydrophilic midline zone and into the hydrophobic region of the coupled membrane. After negative staining or after rotary shadowing of freeze-fractured specimens, these particles were seen to consist of two similar but slightly offset bracket-shaped subunits separated by a small space. Optical analysis confirms this structure. Since the apposing membranes are bracketed or linked by their component particles, the name "bracket junction" is proposed for the complex. Methods are described for isolating a membrane fraction enriched in these junctional complexes; the fraction contains a prominent glycoprotein (mol wt 90,000) as well as a number of other components. The bracket junction is compared with the vertebrate gap junction, in terms of both structure and possible roles in facilitating the permeation of the cell by small molecules.

When magnesium is removed from the culture medium of exponentially growing *Escherichia coli* several changes occur during the early period of starvation. First, the cells become permeable to lactose analogues which cannot be actively transported (3), suggesting that the normal permeability barrier to small molecules imposed by the membrane has been functionally altered. Second, the plasma membrane forms internal 'septate' membranes (14) with a regular spacing of 10 nm. Finally, a regular particle pattern develops in portions of the plasma membrane surface (6). Although there is no direct evidence that these membrane arrays account for the altered permeability properties, they represent a site-specific differentiation with unusual structural properties.

In this paper, I describe the structure of this differentiated membrane in detail and conclude that Mg^{++} starvation in *E. coli* leads to the development of a membrane junction which, like the vertebrate gap junction (8), contains a stable array of intramembranous particles. The structure of this new junction is consistent with the concept (3) that it may confer increased permeability on the *E. coli* cell membrane. I also describe procedures for the isolation of membrane fractions enriched for such junctions; these junctions were analyzed by polyacrylamide gel electrophoresis to deter-

mine the chemical nature of the component membranes. This analysis indicates that the junction particles are composed, at least in part, of a distinct glycoprotein.

MATERIALS AND METHODS

Cultural Conditions

E. coli ML 308-225 (obtained from H. R. Kaback, Roche Institute, Nutley, N.J.) was used in most experiments; all other ML strains were provided by T. H. Wilson (Harvard Medical School, Boston, Mass.). Cells were grown to the early exponential phase at 37°C in glucose-minimal salts medium (6) without iron. To obtain Mg^{++}-starved cells, the bacteria were filtered (Millipore Corp., Bedford, Mass.), washed 3 × in medium without magnesium and resuspended in the same medium at 37°C. After incubation at 37°C for 24 h, Mg^{++}-starved cells were harvested by centrifugation at 10,000 *g* for 5 min at 0°C. Control cells were subjected to similar manipulations in Mg^{++}-containing medium.

Isolation of Cell Membranes

The methods used as described here were modified from Kaback (12). Cells were harvested in the exponential phase ($2–4 \cdot 10^8$ cells per milliliter) or after 24-h starvation by centrifugation at 10,000 *g* for 5 min. The bacteria were washed 2 × in 10 mM Tris, pH 8, and suspended in 33 mM Tris, 20% sucrose. After 1 min, crystalline lysozyme (Sigma Chemical Co., St. Louis, Mo.) was added (0.5 mg/ml). 2 min later, the suspension was diluted 1:10 over a 5-min period with constant stirring, using 100 mM disodium ethylenediaminetetraacetic acid (EDTA), pH 8, at 37°C. After the addition, the temperature was adjusted to 37°C. The cells were quantitatively spherical within 5–10 min and were determined to be free of outer membrane (cell wall) by electron microscopy.[1] These spheroplasts were centrifuged and resuspended in a small volume (1 ml/500 ml culture) of 50 mM potassium phosphate buffer containing 0.1 mM $CaCl_2 \cdot 2H_2O$ and 20% sucrose. They were lysed dropwise, using a syringe and a 23-gauge needle, by diluting 1:80 in 10 mM potassium phosphate buffer, pH 7, at 37°C with stirring. The vesicles were centrifuged at 27,000 *g* for 15 min and treated with nucleases (DNase; RNase; 10 μg/ml) in 50 mM potassium phosphate buffer, pH 7, with 10 mM $MgCl_2$ at 37°C for 20 min. The vesicles were then washed 2 × in 10 mM potassium phosphate buffer (27,000 *g*, 15 min at 0°C) and suspended in 35% (wt/wt) sucrose and run on a step gradient (35, 40, 45, and 50%) in 10 mM potassium phosphate buffer, pH 7, for 2 h at 35,000 rpm (100,000 *g*) with an SW 50 head in a model L ultracentrifuge (Beckman Instruments Inc., Palo Alto, Calif.). Two bands were obtained, one at the 40–45% interface and the other at the 45–50% interface. The buoyant density of the upper 'junction'-enriched band was 1.16–1.18 as determined by isopycnic centrifugation, whereas the lower band containing the cell wall fraction had a density of 1.23–1.24. The isolated membranes or walls were collected dropwise or removed from above, washed 2 × in the appropriate buffer, and subsequently processed in parallel for electron microscopy or electrophoresis.

[1] Control cells formed spheroplasts; Mg^{++}-starved cells formed protoplasts as determined in thin section by electron microscopy. Protoplast formation in normal *E. coli* was brought about by an entirely different set of conditions (Weiss, manuscript in preparation).

Freeze-Cleavage and Etching

Magnesium-starved bacteria were washed 2 × in 10 mM *N*-2-hydroxyethyl-piperazine-*N'*-2"-ethane sulfonic acid (HEPES), pH 7, and infiltrated for 4 h with 20% glycerol at 4°C. Control cells prepared in buffer appear identical to glycerol-treated cells. Glycerol was omitted in etch experiments. A small drop of sample at 23°C was applied to a copper disk and immersed in freezing chlorofluoromethane (Freon 22). Freeze-cleavage and -etching were carried out as described elsewhere (16), using a Balzers unit equipped with electron bombardment guns (Balzers High Vacuum Corp., Santa Ana, Calif.). In some experiments the rotary shadowing technique (4) was used at a low (15°) angle. Replicas were cleaned with Clorox (Procter and Gamble Co., Cincinnati, Ohio), washed with distilled water, mounted on 400-mesh grids, and observed with a Philips 300 electron microscope. Measurements were made directly on the negative in the central area (25 mm diameter) with a Nikon microcomparator (Nikon Inc., Instrument Div., EPOI, Garden City, N. Y.).

Thin Sectioning

Intact cells were fixed in the phosphate-buffered glutaraldehyde-osmium tetroxide described by Schnaitman (18). Membrane fractions were prepared for thin sectioning as follows: Samples were washed 2 × in HEPES buffer, pH 7, and fixed in HEPES-buffered 3% glutaraldehyde for 2 h at 0°C. After fixation, the samples were washed 3 × in HEPES buffer and transferred to 1% OsO_4 in HEPES and fixed for 2 h at 0°C. The OsO_4 was washed out with three changes of HEPES, and the sample was then dehydrated in ethanol and embedded in Araldite 502. Silver-to-grey sections were cut on a Reichert ultramicrotome (American Optic Corp., Buffalo, N. Y.), mounted on 400-mesh grids and stained with 2% uranyl acetate and lead citrate.

Negative Staining

Membranes were applied to a thin film of carbon on uncoated 400-mesh grids. Specimens were rinsed with distilled water, stained with 1% uranyl acetate (pH 4.6), and air dried.

Image Enhancement

Laser diffraction patterns of arrays (kindly prepared by Tim Baker, University of California, Los Angeles, Calif.) were filtered through a mask and recombined to provide a final image which was then recorded on 35-mm film.

SDS-Polyacrylamide Gel Electrophoresis

Slab gel electrophoresis was carried out as described by Ames (1). Slab gels were stained for protein by the method of Fairbanks et al. (5), using a rotator to accelerate penetration and diffusion. Cylindrical gels were stained for 12 h with 0.05% Coomassie Blue in 35% TCA. Destaining was done with 7% HAc followed by 10% isopropanol-10% HAc. Companion gels were stained for carbohydrate by the periodic-acid-Schiff (PAS) method (5). Gels were scanned with a Zeiss PMQ II spectrophotometer (Carl Zeiss Inc., New York, N. Y.) with a linear transport and Sargent recorder (R. L. Sargent Co., Houston, Texas). For quantitation of polypeptides, peaks were cut out and weighed with a Mettler balance (Mettler Instrument Corp., Princeton, N. J.).

RESULTS

E. coli Membrane Junctions

When Mg^{++}-starved *E. coli* membranes fold back on themselves, the two cytoplasmic surfaces form a novel type of membrane junction. These are most directly visualized when the membranes from such cells are isolated and examined in thin section. The resulting images are shown in Fig. 1 in which two closely apposed membranes (*M1*, *M2*, Fig. 1, inset) are seen with a dense midline zone (*MLZ*) in between. Fig. 2 illustrates the features of this zone in oblique section. Here, one sees parallel rows separated by thin, regularly spaced lines. No such images are seen when normal *E. coli* membranes are isolated.

Visualization of these junctions *in situ* is best accomplished by freeze-fracture followed by rotary shadowing of cross-fractured frozen cells. This is shown in Fig. 3. Here, again, one sees two closely apposed membranes with a central zone in between. As with thin sections, the features of the junction depicted here (Fig. 3, inset) are the cell membrane (*M1*), the midline zone (*MLZ*) and the coupled membrane (*M2*).

When cells are fixed and examined in thin section, the midline zone of the junction is particularly distinct. In Fig. 4, this zone appears as a row of well-defined particles. The other components of the junction illustrated here are the cell membrane (*M1*) and the coupled membrane (*M2*).

Internal Junction Structure

Freeze-fracture rotary shadowing also permitted a limited view of the internal structure of the apposed membranes. In Fig. 5, for example, the midline zone of the junction (*MLZ*) is seen to correspond with an internal array of intramembrane particles (*M1*, A-face).[2]

More extensive views of these internal faces were obtained in replicas where the fracture plane passed through the membrane interior. Fig. 6 is a particularly favorable replica in that it shows both developing and mature particle arrays. Shortly after transfer to Mg^{++}-free medium, small 'initiation sites' (Fig. 6, *I*) are detected within the membrane: Intramembranous particles, smaller than those encountered in the surrounding membrane, cluster to form a few short parallel rows of particles (Fig. 6, *I*). Such developing sites continue to form throughout the starvation period while others go on to mature. The A (cytoplasmic) face of a mature array is also shown in Fig. 6. Extensive parallel rows of particles are now present and are oriented approximately 45° with respect to the cell axis. Fig. 7 shows the B (external) face of a mature array: Its lattice imprint of particle pits is complementary to the particle arrays of the A-face.

I occasionally observed images such as that depicted in Fig. 8 where the fracture plane jumps so as to produce a regular alternation of particulate and smooth faces. This fracture pattern presumably results when the fracture plane travels through a multi-layered region such as that depicted in Fig. 3 (arrow). Fig. 8 depicts the A-faces and Fig. 9 shows the B-faces observed in such regions. This kind of alternating fracture pattern occurs in other junctions as well (8).

Freeze-Etched Membranes

The surface of membrane junctions such as that illustrated in Fig. 11 can be visualized by freeze-etching; isolated membranes proved to be the best material for this. As seen in Fig. 12, a smooth surface is associated with the A-face of the cell membrane (*M1*); a smooth surface is also associated with the B-face of the coupled membrane (*M2*) (not shown). Therefore, while the A-face particles of M1 appear to extend through the midline zone into the coupled membrane (Fig. 9), no evidence of extension to either surface was found.

---

[2] A diagrammatic representation of Figs. 5–9 is illustrated in Fig. 10.

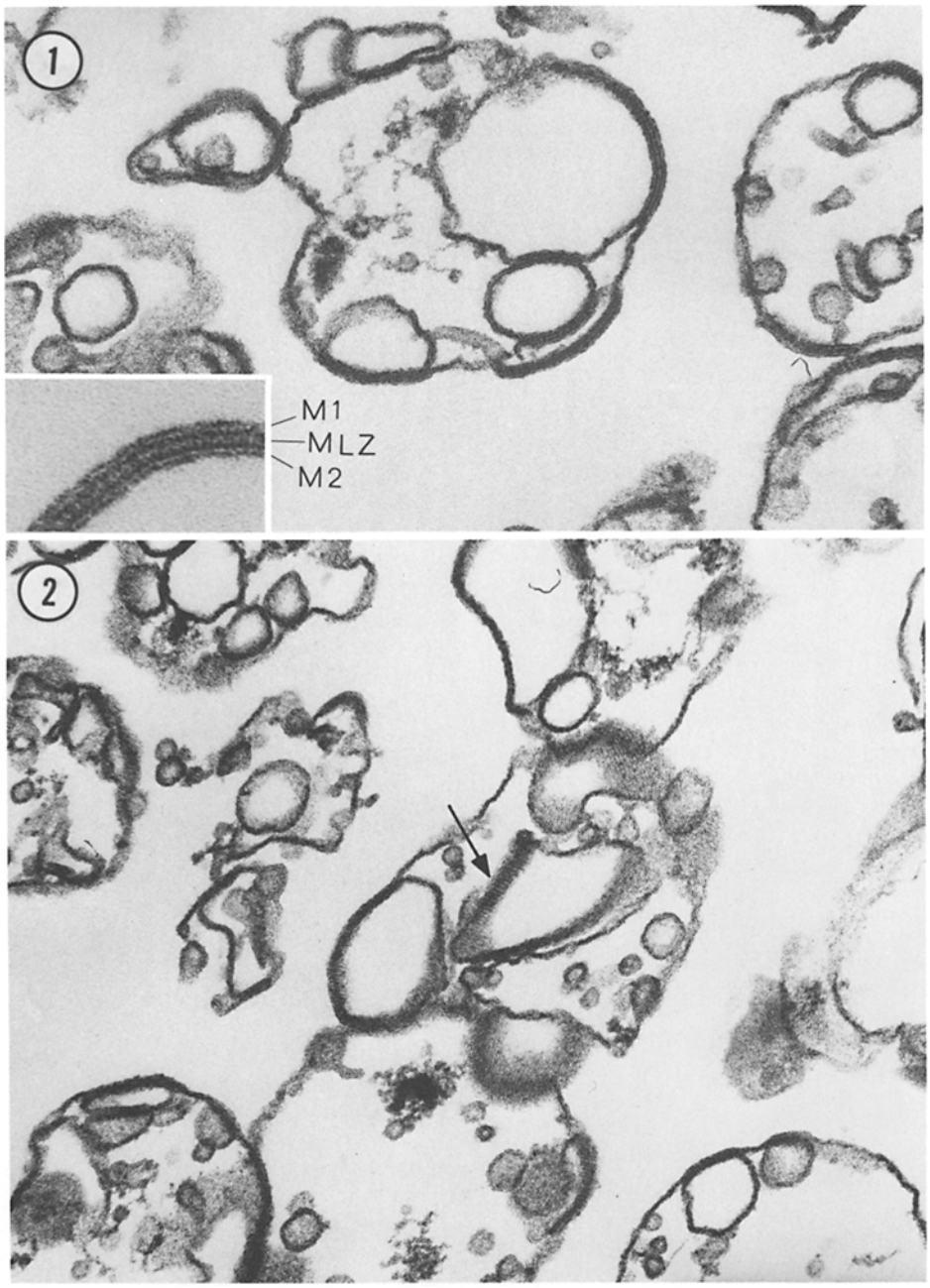

FIGURE 1 Membrane junction isolated from Mg^{++}-starved *E. coli:* the cell membrane (*M1*) and the coupled membrane (*M2*) are joined by a dense layer, the midline zone, *MLZ* (inset). × 78,000; inset × 200,000.

FIGURE 2 Isolated membrane junction visualized in oblique section. Parallel rows of translucent material are seen (arrow). They are separated by thin dense lines. × 65,000.

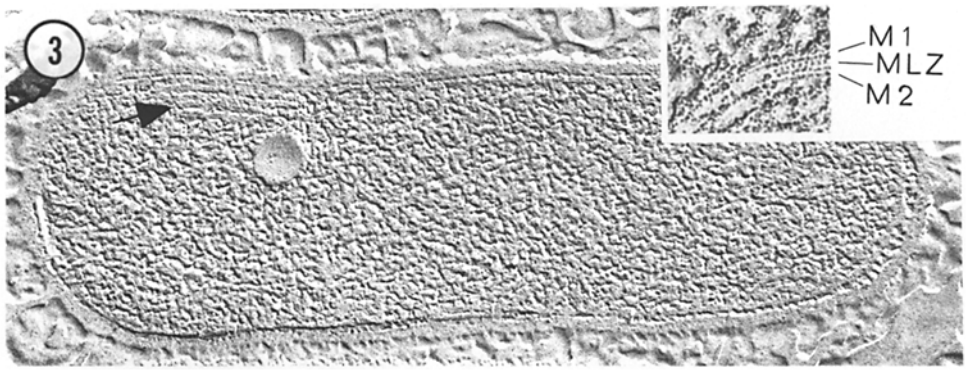

FIGURE 3 Multilayered region of membrane junctions (arrow) visualized in freeze-fractured whole cells. Rotary shadowing (inset) shows that each junction consists of the cell membrane (*M1*), the midline zone (*MLZ*) and the coupled membrane (*M2*). × 78,000; inset, × 150,000.

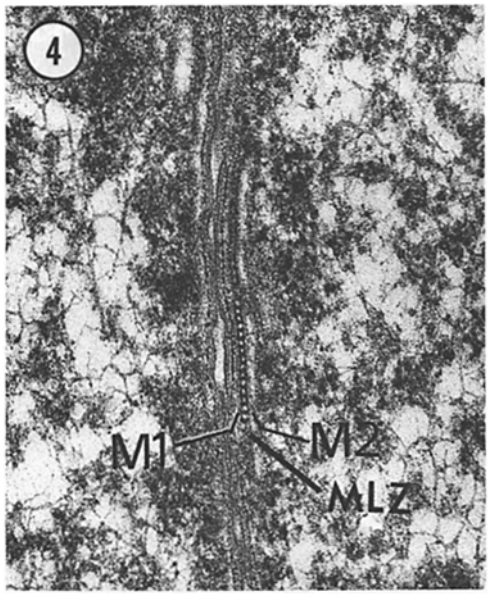

FIGURE 4 Membrane junction seen in a fixed and sectioned cell. The midline zone (*MLZ*) of the junction appears as a row of regularly spaced particles between the cell membrane (*M1*) and the coupled membrane (*M2*). × 94,000.

Membrane Particle Substructure

The structure of junction particles *in situ* was observed by rotary shadowing of freeze-cleaved cells. As illustrated in Fig. 13, the A-face particles carry two subunits separated from each other by a small space. In cases where the particles are shadowed from all sides as in Fig. 14, they often appear doughnut shaped. Image enhancement of such regions indicates that the particles are not doughnut shaped.

Negatively stained specimens were used to visualize the detailed structure of particles in isolated *E. coli* membrane junctions. In the resulting images, individual particles commonly appear to be divided into two equal but slightly offset bracket-shaped subunits (Fig. 15). The central deposit of stain between the subunit pairs is highly contrasted, suggesting deep penetration. This penetration is suggestive of a central depression or furrow.

Rotary shadowed and negatively stained preparations can be compared directly with each other. Isolated arrays that had separated into rows provided the best negatively stained material for such a comparison. The appearance of individual rows such as those illustrated in Fig. 16 is similar to that of closely packed rows in Fig. 13. Continuing on to the particles in these rows, a direct comparison of particle structure (Fig. 13, inset, and Fig. 16, inset) may be made on a point-to-point basis, using individual subunits and the space between them. Such a comparison points to similarities between negatively stained and rotary shadowed particle substructure. Similar comparisons made with optically filtered images (Figs. 17 and 18) support the agreement between the average images of negatively stained and rotary shadowed junction particles. In addition, particles visualized by negative staining have the same dimensions (Table I) as those observed by rotary shadowing of freeze-cleaved cells.

Profile views of negatively stained particles were encountered when a junction was oriented

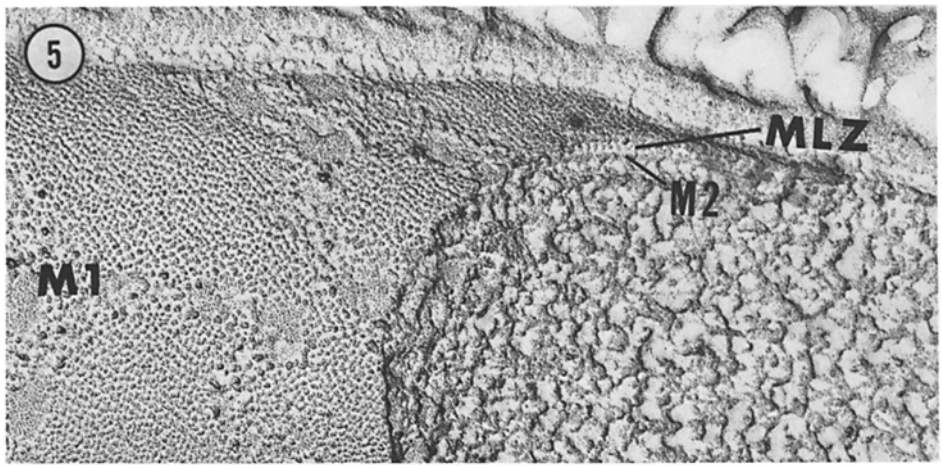

FIGURE 5 Internal junction structure showing the A-face of the cell membrane (*M1*) and the midline zone (*MLZ*). The position of the coupled membrane (*M2*) is marked. × 125,000.

perpendicular to the grid as in Fig. 19. With such images, it was possible to estimate particle height which showed good agreement with the value obtained from the midline zone in cross-fractured junctions (Table I). The other measurements of particle dimension seem to indicate that negatively stained rows of particles are equivalent to the rows visualized in fixed and sectioned material (Fig. 2).

In view of the distinctive structure of particle subunits, I propose the name 'bracket junction' for the intramembranous particle array. This term describes the 'bracketing' or linking of the apposing membranes by the component particles.

Effect of Growth Stage on Junction Morphology

The extensive development of bracket junctions described above occurs when cells in the early exponential stage of growth are transferred to Mg^{++}-free medium. If cells are instead transferred to Mg^{++}-free medium at the mid-exponential phase or later, bracket-junction formation is greatly reduced. Instead, large areas without particles appear in longitudinal fractures of such cells after 24 h without Mg^{++} (not shown).

Gel Electrophoresis of Whole Cells

The polypeptide composition of various ML strains of *E. coli* is shown in Fig. 20, where each lane displays the electrophoretic patterns of 15 μg of protein from cells at mid-exponential phase (2×10^8 cells/ml). An obvious difference is evident when the control cells (samples 2–6) are compared with the corresponding patterns of cells starved for Mg^{++} (samples 7–11): a new band appears in starved cells at a position corresponding to a molecular weight of 90 kdaltons. This band is particularly evident when samples 11 (*E. coli* ML 308-225, Mg^{++}-starved) and 12 (normal control) are compared directly. A second visible difference is the intensity of the band at 15 kdalton (arrow, Fig. 20). A third difference is that in Mg^{++}-starved cells (samples 7–11) two high molecular weight bands, one on each side of the 90-kdalton band, also seem to be lost.

The highest level of the 90-kdalton band appeared in *E. coli* ML 308-225, and all subsequent studies were done with this strain. The appearance of the 90-kdalton band is first noted in this strain after about 4 h of starvation; in parallel experiments, small initiation sites of particle arrays (Fig. 6) were first seen in fractured cells at about 6 h. The increase in the cell-surface area occupied by the particle arrays during the subsequent starvation period correlates directly with an increased level of the 90-kdalton band.

The relative apparent enrichment of cells for the 90- or the 15-kdalton band was dependent on the conditions of starvation: in cells starved from mid-exponential phase (Fig. 20) a high level of the 15-kdalton protein was observed, whereas when cells were starved from early exponential phase the level of the 90-kdalton protein was increased compared with the 15-kdalton protein. Fig. 21 shows the gel pattern of the control (sample 1) and

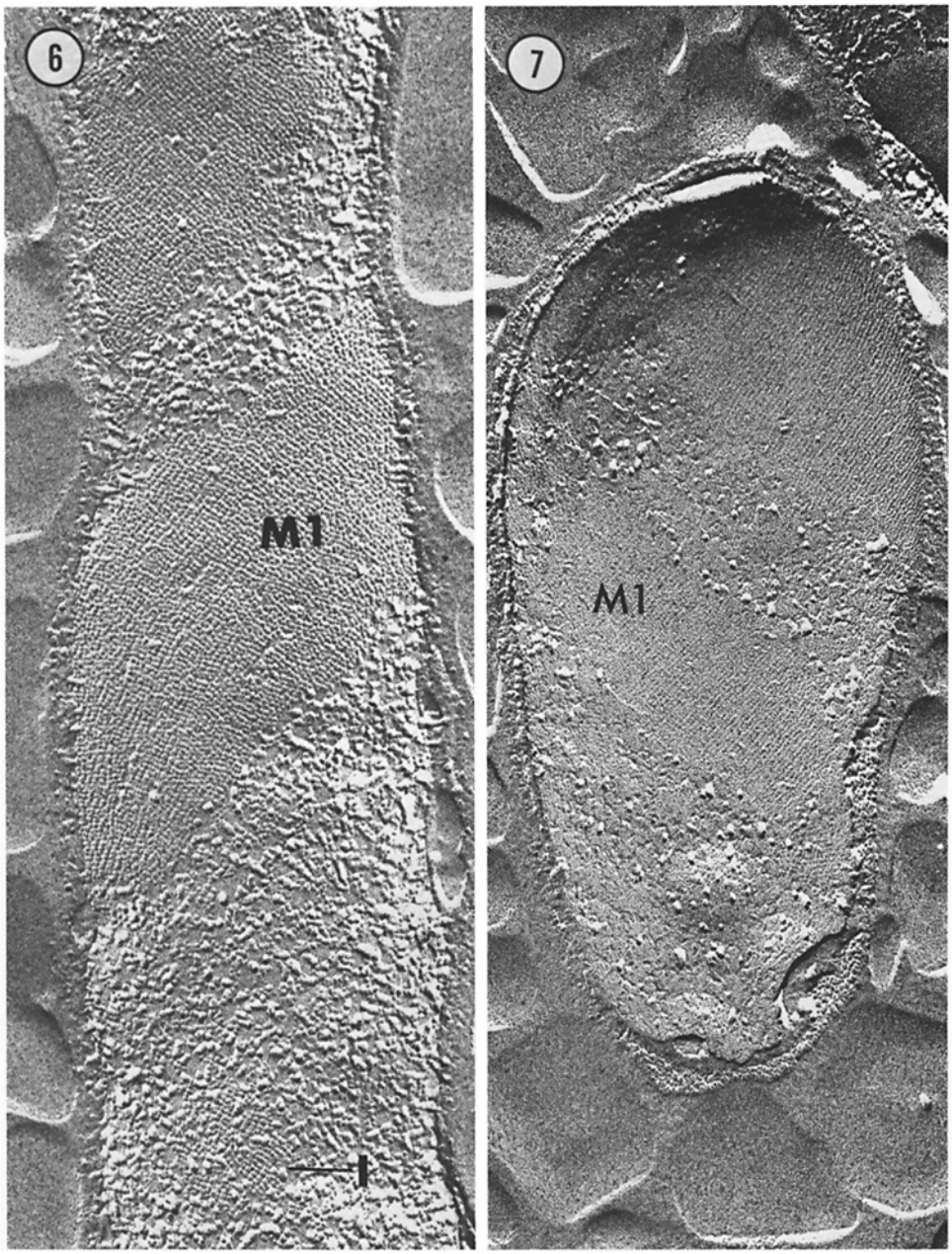

FIGURE 6 Internal features of developing and mature junctions. Small initiation sites (*I*) mark the early stages of junction formation; these sites form mature particle arrays in the A-face of the cytoplasmic membrane (*M1*). × 100,000.

FIGURE 7 Mature array in B-face of the cell membrane (*M1*), showing a lattice of particle pits. Imprint pattern corresponds with particle pattern of A-face. × 100,000.

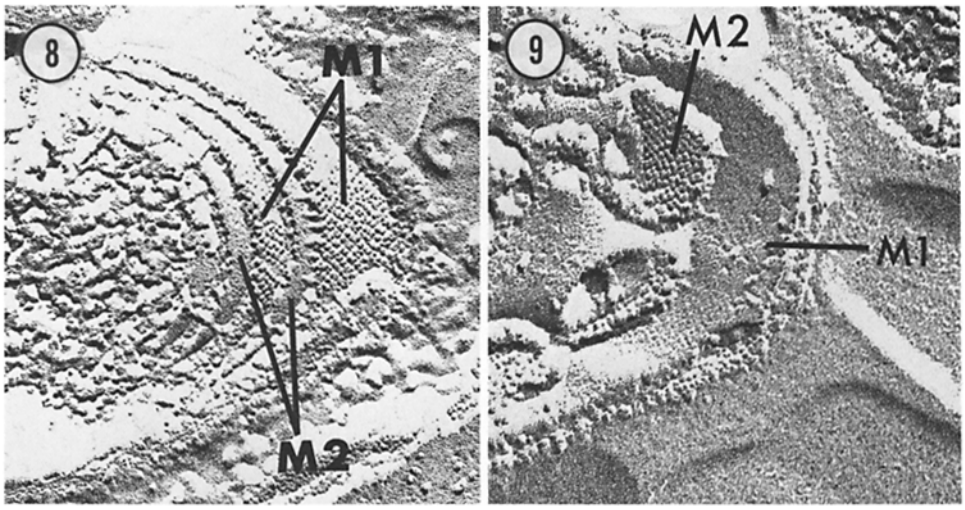

FIGURE 8 Multilayered junctional region. The A-faces are seen after the fracture alternates through the cell membrane (*M1*) and the coupled membrane (*M2*). × 140,000.

FIGURE 9 The B-faces of a membrane junction. The cell membrane (*M1*) and the coupled membrane (*M2*) are visualized. × 140,000.

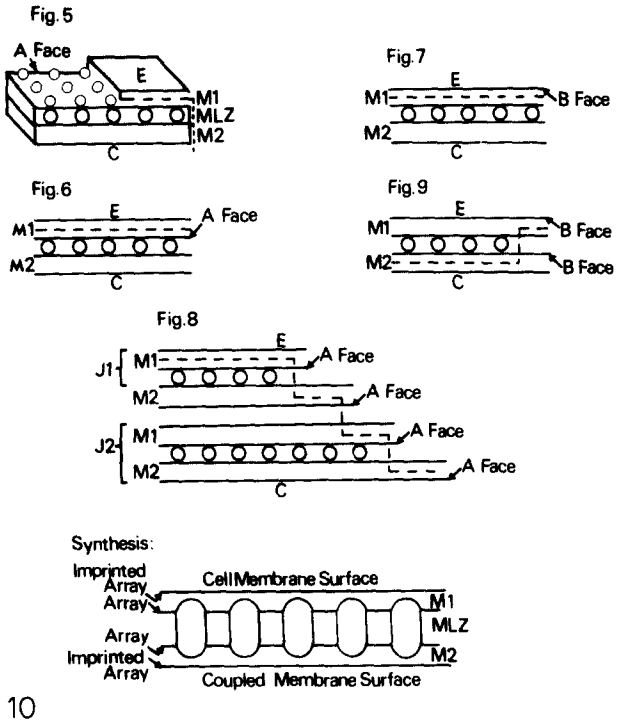

FIGURE 10 Diagrammatic representation of cleavage planes in junctions illustrated in Figs. 5–9. Each membrane can be split into two monolayers. The location of the cleavage plane is indicated by a dashed line. Two junctions are visualized in Fig. 8. The synthesis of the figures illustrated indicates the type of surface exposed by cleavage. An array of particle pits occasionally visualized on the A-face of the coupled membrane is included in the synthesis. The outer membrane surfaces are marked. *E*-extracellular, *C*-cytoplasm, *J*-junction, *M1*-cell membrane, *M2*-coupled membrane, *MLZ*-midline zone.

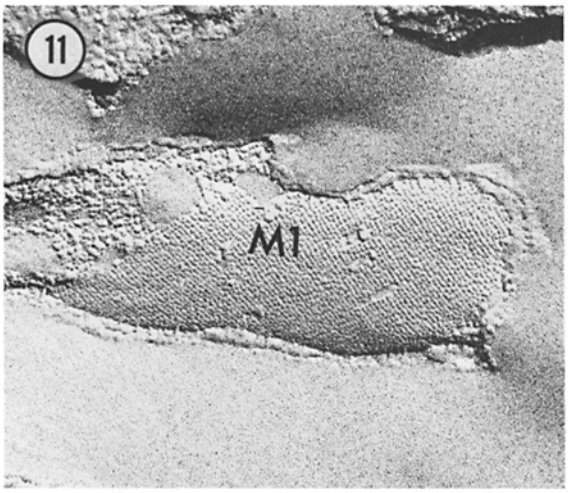

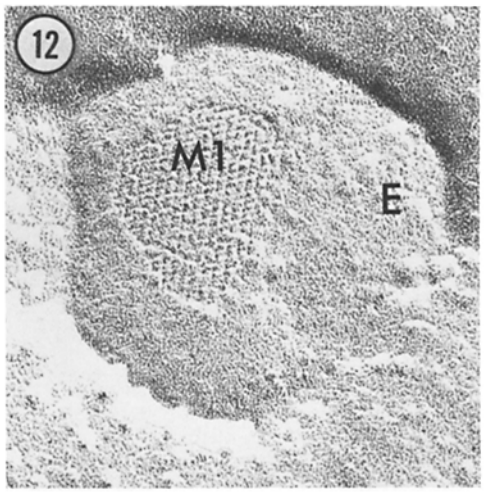

FIGURE 11 Mature membrane array in A-face of the cell membrane *M1*. Cell frozen in 10 mM HEPES buffer; freeze-cleaved, no etching. × 94,000.

FIGURE 12 Etched surface (*E*) of isolated membrane junction. The A-face of the cell membrane (*M1*) is seen. Cell frozen in 10 mM HEPES buffer. × 150,000.

TABLE I

*Dimensions of Membrane Junctions**

	Particle diameter	Particle height	Row to row	Center to center	Subunit dimension	Core dimension	Junction width
Negative staining	55 × 66 (85)‡	47	84 (74)	63 (86)	25 × 55	16 × 55 (20–25)	–
Rotary shadowing	52 × 64	48	84	65	24 × 51	12 × 51	257
Freeze-fracture	52 × 63 (80–90)	–	80	66	–	–	196
Thin sectioning	–	72	90	–	–	–	192 (150)

* Values given in angstroms for bracket junction particles
‡ Vertebrate gap junction values (8) in parenthesis

Mg^{++}-starved cells (sample 2) derived from an early starvation. The high level of the 90- relative to the 15-kdalton band is particularly striking here.

Gel Electrophoresis of Isolated Membranes

The purification of membranes from control and Mg^{++}-starved cells was followed by SDS-gel electrophoresis. Fig. 22 presents the results from one experiment in which the proteins of intact cells, cell walls, and cell membrane fractions were compared. About 15 μg of protein was applied to each gel, so that the relative intensity of proteins in isolated cell walls and membranes could be compared directly. The 90-kdalton protein is found to account for about 35% of the total protein while the 15-kdalton band accounts for 13% of the protein in these isolated membranes as calculated from gel scans in experiments with Coomassie Blue-stained cylindrical gels.

When identical disk gels of the membrane fraction isolated from Mg^{++}-starved cells were stained for protein and carbohydrate (Fig. 23), a major PAS-positive band ran adjacent to the 90-kdalton protein, whereas control membranes showed only traces of low molecular weight PAS-positive bands. The PAS-positive band had the same shape as the protein band, both bands having a characteristic feathered edge on the trailing end of the band. A second minor doublet band was observed

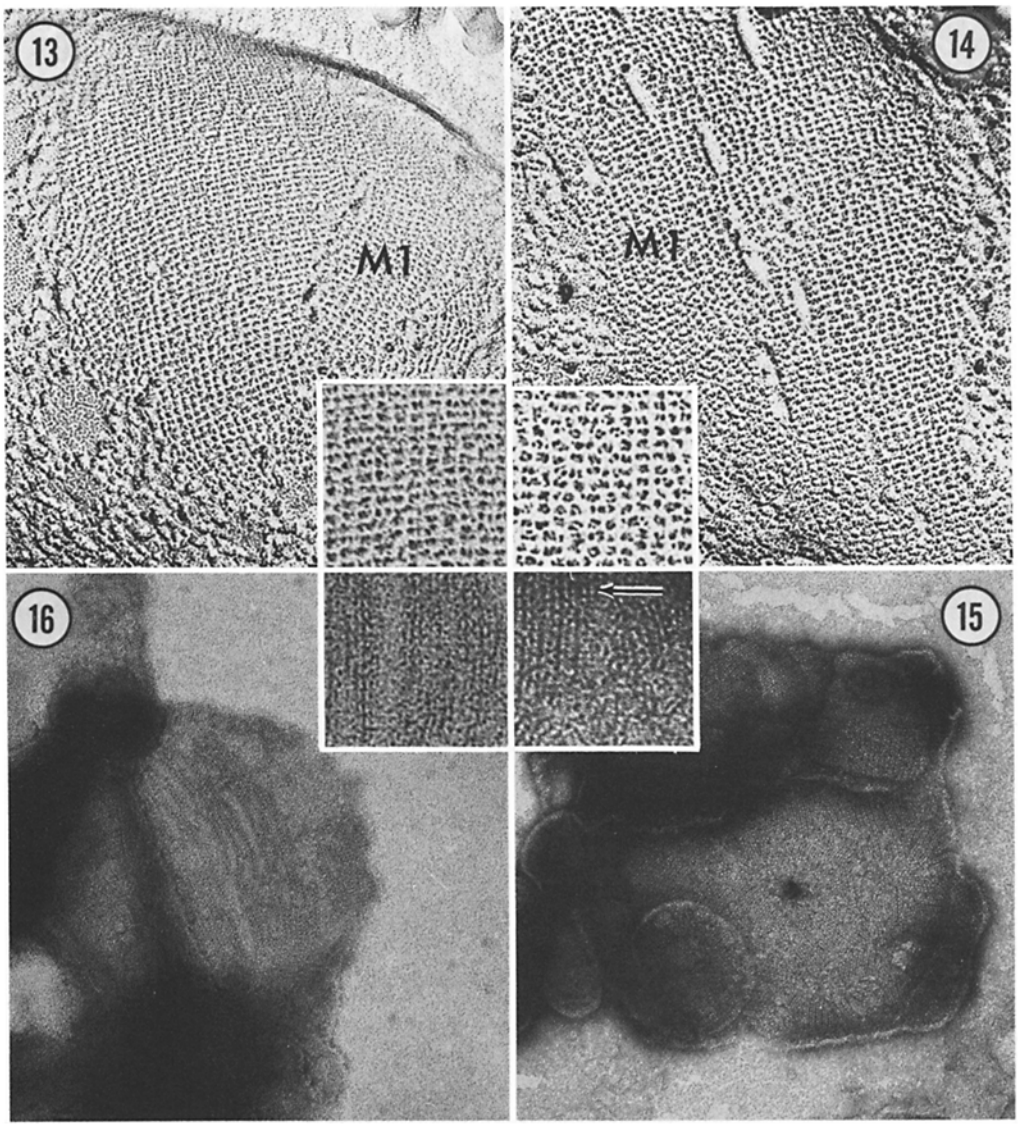

FIGURE 13 Junction particles visualized by rotary shadowing of the cell membrane (*M1*). A-face particles (inset) carry two subunits separated by a small space. × 150,000; inset × 250,000.

FIGURE 14 Junction particles of the cell membrane (*M1*) visualized by rotary shadowing of freeze-fractured cells. Doughnut-shaped particles are visualized (inset). × 150,000; inset × 250,000.

FIGURE 15 Negatively stained membrane junction. The subunit pair (inset; indicated by arrow) is separated by a deposit of stain. × 78,000; inset × 250,000.

FIGURE 16 Negatively stained rows of junction particles. Each subunit pair is separated by a small space filled with stain (inset). × 78,000; inset × 250,000.

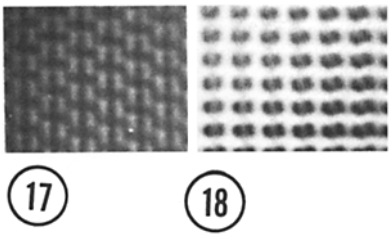

FIGURE 17 Negatively stained bracket junction particles. After optical filtration, isolated junction particles are visualized as elongated units separated by a central stain-filled line.

FIGURE 18 Freeze-cleaved and rotary shadowed bracket junction particles. Junction particles *in situ* carry two subunits separated by a central depression. (Prepared by Tim Baker.)

with a slightly lower molecular weight in the PAS gel. Although no comparable component is seen in the disk gel stained for protein (Fig. 23), the increased resolution in slab gels indicates that this component may correspond to a doublet band (*DB*) observed most clearly in lane 2 of Fig. 21 and shown to be a component of the membrane fraction (lane 6, Fig. 22). Additional gels containing 5% acrylamide were prepared with the same membrane preparation shown in Fig. 22, and it was found that the 90-kdalton protein again had the same electrophoretic mobility as the major PAS band. Its electrophoretic behavior is thus consistent with that of a single glycoprotein component.

DISCUSSION

Comparison with Vertebrate Gap Junction

The particle arrays that accumulate within the cell membrane of *E. coli* during bracket junction formation are reminiscent of those of vertebrate gap junctions in morphology. Thus, both types of junctions are visualized in section as closely apposed bilayer pairs with distinct material in the midzone between the membranes. In negatively stained images, both appear to have a regular array of particles with a central deposit of stain. Similarly, after freeze-cleavage, both of them appear to have an orderly array of particles which differ in size from the surrounding membrane particles. In view of these morphological similarities, it is of some interest to compare the two kinds of membrane junctions in terms of their development and their presumed functional roles.

In the case of gap junction development, the mechanism of assembly is thought to involve rapid lateral movement (15) of particles within the bilayer since the small formation plaque precursors of mature gap junctions can develop within 5–30 min in reaggregated Novikoff hepatoma cells (11). Bracket junction development in *E. coli*, of course, proceeds under quite different constraints; a critical level of Mg^{++} starvation must first be attained and small junctional areas reminiscent of formation plaques do not appear until Mg^{++} starvation has progressed for 6 h. The junctional areas then continue to increase in size as starvation proceeds, suggesting that the rate-limiting step involves the formation of the 50-Å junction particles and not their lateral aggregation. My observations do not reveal whether the junction particles are formed *de novo* or are manifestations of preexisting membrane components, but, whichever is the case, preexisting particles clearly must be modified and/or moved. An attractive model is one that assumes that the larger 85-Å particles represent precursors for the 50-Å junction particles and that the existing particles are modified by glycosylation (an economical mode for junction formation). The accumulation of particles in the junction most likely involves pairs of particles con-

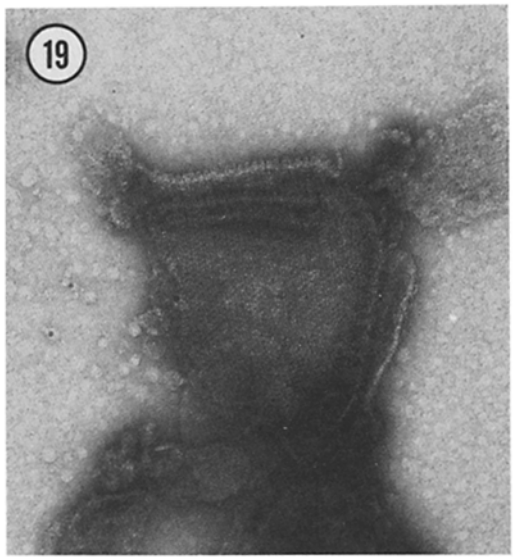

FIGURE 19 Profile of negatively stained junction particles. Membrane particles extend away from folded edge of the junction visualized here. × 140,000.

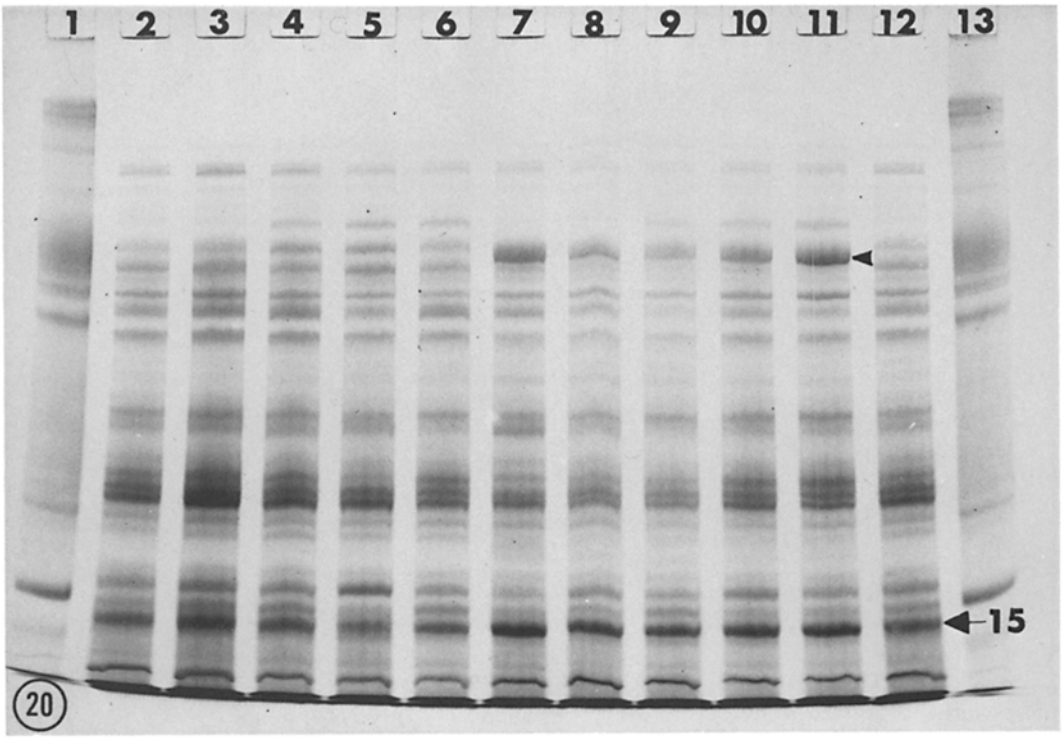

FIGURE 20 Comparison of normal and Mg^{++}-starved *E. coli*. Various ML strains were grown to mid-exponential phase (2×10^8 cells/ml) and starved for 24 h (see Methods). Samples at each end are despectrinated red blood cell ghosts. Each sample contains about 15 μg protein. Samples 2–6 are controls, sample 2, ML 3, sample 3, ML 30, sample 4, ML 35, sample 5, ML 308, sample 6, ML 308-225. Samples 7–11 are Mg^{++}-starved cells in the following order: ML 3, ML 30, ML 35, ML 308, ML 308-225. Sample 12 is control ML 308-225 and may be compared directly with sample 11. Arrow points to the 90-kdalton polypeptide which appears in Mg^{++}-starved cultures. Samples 7–11 also show an increase in the 15-k dalton band. Acrylamide concentration was 8%.

nected across the intermembrane space which ultimately forms the midline zone.

The presumed functional role of the vertebrate gap junction in a tissue is to provide low-resistance pathways between adjacent cells which could serve as channels for 'cross-feeding' and/or intercellular communication (13). 'Intercellular' features of the *E. coli* bracket junction do not exist, of course, but the junctions could serve to confer altered permeability properties on the *E. coli* cell itself. This hypothesis is consistent with the increased permeability to small molecules observed in Mg^{++}-starved *E. coli* (3).

Comparison with Mitochrondrial Junctions

Recent studies performed on mitochondria isolated from striated muscle and other tissues have shown that, after isolation, membrane junctions formed between the crystal membranes or between the outer and inner mitochondrial membranes (17). The similarity in structure between mitochondrial junctions and the bracket junction is of interest in view of the mode of formation of both junctions. Visualization of mitochondrial junctions begins after isolation and depends on storage of tissue. This dependency seems analogous to Mg^{++} starvation in which a specific deficiency leads to the development of a specific membrane modification.

Chemical Nature of Bracket Junction Particles

The bracket junctions appear to contain identical membrane particles which differ from nonjunc-

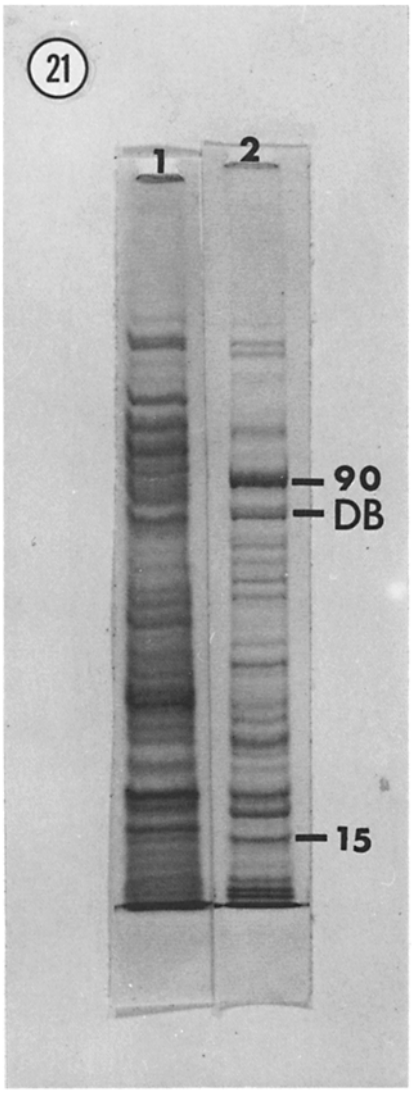

FIGURE 21 Electrophoresis of *E. coli* starved from early exponential phase. Sample 1, normal cells; sample 2, Mg^{++}-starved cells. The relative amount of the 90-kdalton component is increased in these cells. The intensity of the 15-kdalton polypeptide is decreased. Acrylamide concentration was 8%. The doublet band (*DB*) is visualized.

tion particles; it is therefore reasonable to expect that they are comprised of distinct polypeptides. The fact that a new 90-kdalton polypeptide appears in *E. coli* at about the time that bracket junctions first appear and that this polypeptide increases as the particles increase in number suggests that this polypeptide may be a major component of the membrane particle, a suggestion supported by the fact that isolated membranes enriched for bracket junctions are enriched for the same 90-kdalton macromolecule. Correspondingly, a lower level of the 90-kdalton polypeptide appears in late log cells when bracket junctions are decreased. The 90-kdalton component is shown to be a glycoprotein, which is similar to other membrane proteins (10, 16) but not, apparently, to gap junction proteins (7).

The probable association of two other components with bracket junction particles should also be mentioned. The first component is a prominent polypeptide with a molecular weight of 15 kdaltons. The low molecular weight of this band suggests that there may be at least as many copies of this component as there are of the 90-kdalton band. If a 1:1 (90:15 kdalton) relationship does exist, an association of the 15-kdalton band with the bracket junction particles would be quite likely. The second component is a glycoprotein doublet band that represents a small amount of the carbohydrate detected. Since a doublet band which may correspond to the glycoprotein appears in the membrane fraction of Mg^{++}-starved cells, it seems possible that this band could represent some minor component of the bracket junction.

CONCLUSION

In addition to the vertebrate junctions mentioned above, bracket junctions also seem homologous to the infolded and closely apposed membranes in photosynthetic bacteria (reviewed in 9), but, in this case, as with wall-membrane adhesions in normal *E. coli* (2), freeze-cleave electron microscopy has not shown similar structural differentiations. Thus, the synthesis of bracket junctions is not simply a response to the infolding of the plasma membrane but appears to involve at least two factors: cellular degradation and alteration of membrane proteins. Whether the alteration of membrane proteins reflects synthesis of new polypeptides or modification of preexisting ones cannot be distinguished by the experiments reported here.

In either case, it seems clear that bracket junction particles are comprised of a limited number of components, one of which is a distinct glycoprotein.

The assistance of Blue Tabor, G. Miller, and Naomi Buklad is acknowledged.

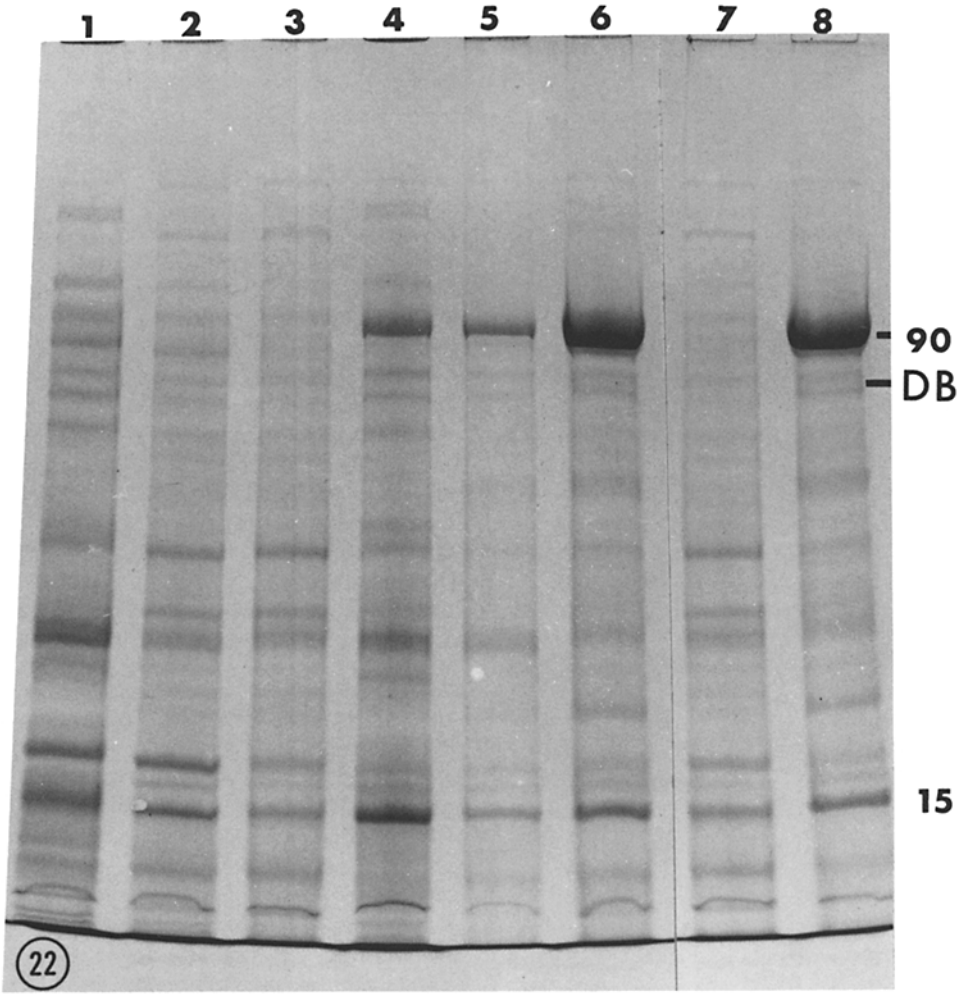

FIGURE 22 Comparison of Mg^{++}-starved and control cell fractions. Cells were grown to 2×10^8 bacteria/ml and starved for 24 h until a cell concentration of 2×10^8 cells/ml. Control cells sampled at 2×10^8/ml. Samples 1, 2, 3 are control cells, cell walls and cell membranes. Samples 4,5,6 are Mg^{++}-starved cells, cell walls and cell membranes. Samples 7,8 control membranes, Mg^{++}-starved membranes, may be compared directly. Doublet band (*DB*) is also seen.

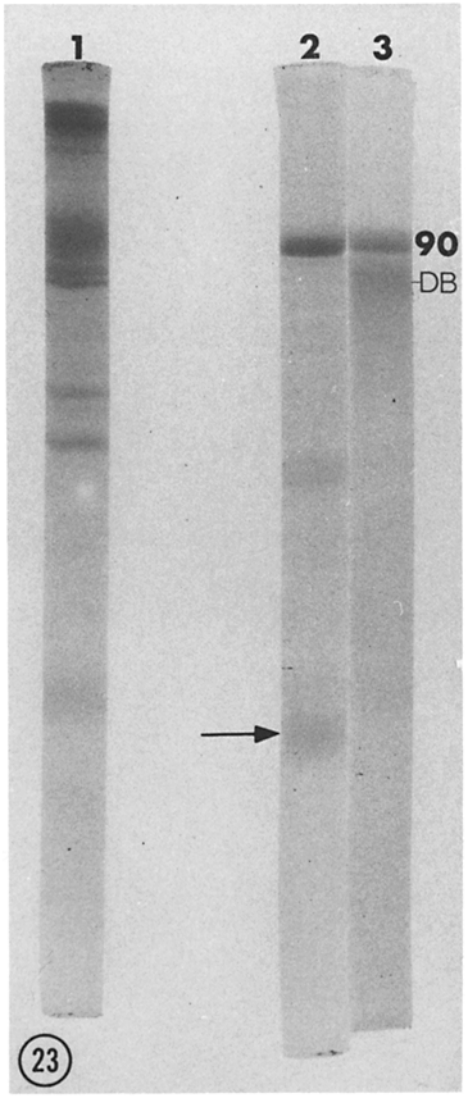

FIGURE 23 Bracket junction membrane fraction. Sample 1, human erythrocyte ghosts; sample 2, Coomassie Blue-stained membranes; sample 3, PAS-stained membranes. The 90-kdalton band appears in Coomassie Blue- and PAS-stained gels. The doublet band (*DB*) in PAS-stained gel is not resolved in the Coomassie Blue gel. The 15-kdalton band appears at arrow.

R. Weiss was supported by a postdoctoral fellowship (PF876) from the American Cancer Society. Support was also provided by National Institutes of Health and National Science Foundation grants to D. Branton.

Received for publication 26 November 1975, and in revised form 3 January 1977.

REFERENCES

1. AMES, G. F.-L. 1974. Resolution of bacterial proteins by polyacrylamide gel electrophoresis on slabs. *J. Biol. Chem.* **249**:634–644.
2. BAYER, M. E. 1968. Areas of adhesion between wall and membrane of *Escherichia coli*. *J. Gen. Microbiol.* **53**:395–404.
3. BROCK, T. D. 1962. Effects of magnesium ion deficiency on *Escherichia coli* and possible relation to the mode of action of novobiocin. *J. Bacteriol.* **84**:679–682.
4. ELGSAETER, A. 1974. Ph.D. Dissertation. University of California, Berkeley, Calif.
5. FAIRBANKS, G., T. L. STECK, and D. F. H. WALLACH. 1971. Electrophoretic analysis of the major polypeptides of the human erythrocyte membrane. *Biochemistry*. **10**:2606–2617.
6. FIIL, A., and D. BRANTON. 1969. Changes in the plasma membrane of *Escherichia coli* during magnesium starvation. *J. Bacteriol.* **98**:1320–1327.
7. GOODENOUGH, D. A. 1974. Bulk isolation of mouse hepatocyte gap junctions. *J. Cell Biol.* **61**:557–563.
8. GOODENOUGH, D. A., and J.-P. REVEL. 1970. A fine structural analysis of intercellular junctions in the mouse liver. *J. Cell Biol.* **45**:272–290.
9. GOODENOUGH, U. W., and L. A. STAEHELIN. 1971. Structural differentiation of stacked and unstacked chloroplast membranes. *J. Cell Biol.* **48**:594–619.
10. HONG, K., and W. L. HUBBELL. 1972. Preparation and properties of phospholipid bilayers containing rhodospin. *Proc. Natl. Acad. Sci. U. S. A.* **69**:2617–2621.
11. JOHNSON, R., M. HAMMER, J. SHERIDAN, AND J.-P. REVEL. 1974. Gap junction formation between reaggregated Novikoff hepatoma cells. *Proc. Natl. Acad. Sci. U. S. A.* **71**:4536–4540.
12. KABACK, H. R. 1971. Bacterial membranes. *Methods Enzymol.* **22**:84–120.
13. LOEWENSTEIN, W. R. 1966. Permeability of membrane junctions. *Ann. N. Y. Acad. Sci.* **137**:441–472.
14. MORGAN, C., H. S. ROSENKRANZ, B. CHAN, AND H. M. ROSE. 1966. Electron microscopy of magnesium depleted bacteria. *J. Bacteriol.* **91**:891–895.
15. PINTO DA SILVA, P. 1972. Translational mobility of the membrane intercalated particles of human erythrocyte ghosts. *J. Cell Biol.* **53**:777–787.
16. PINTO DA SILVA, P., and D. BRANTON. 1970. Membrane splitting in freeze-etching. *J. Cell Biol.* **45**:598–605.
17. SAITO, A., M. SMIGEL, AND S. FLEISCHER. 1974. Membrane junctions in the intermembrane space of mitochondria from mammalian tissues. *J. Cell Biol.* **60**:653–663.
18. SCHNAITMAN, C. A. 1970. Protein composition of the cell wall and cytoplasmic membrane of *Escherichia coli*. *J. Bacteriol.* **104**:896–904.